ELSEVIER

Contents lists available at ScienceDirect

Bone Reports

journal homepage: www.elsevier.com/locate/bonr



Ribosylation-induced increase in advanced glycation end products has limited impacts on mechanical properties in human cortical bone

Katelynn R. Gallagher, Olivia N. White, Andrew A. Tomaschke, Dyann M. Segvich, Joseph M. Wallace *

Weldon School of Biomedical Engineering, Department of Purdue University, 723 W Michigan St (SL220), Indianapolis, IN, USA 46202

ARTICLE INFO

Keywords: Diabetes Microcomputed tomography Dynamic mechanical analysis Ribose/ribosylation Fluorescence

ABSTRACT

Diabetes affects over 38 million individuals in the U.S. and is associated with a heightened risk of fractures despite normal or elevated bone mineral density (BMD). This increased fracture susceptibility may be linked to the accumulation of advanced glycation end products (AGEs), which are theorized to compromise bone quality by stiffening the collagen network, leading to tissue embrittlement. In this study, the mechanical effects of AGE accumulation in human cortical bone were evaluated *in vitro*. Bone beams, derived from a human femur, were incubated in a ribose solution to induce AGE accumulation, while control beams were incubated in a control solution. Dynamic Mechanical Analysis (DMA) and three-point bending tests were conducted to assess the mechanical properties of the bone beams. Fluorescent AGE analysis was performed to quantify and compare AGE levels between the groups. The study found no significant differences in mechanical properties between the control and ribose-treated groups, despite a significant elevation in normalized AGE content in the ribose group. These results suggest that AGE accumulation may have a weaker impact on the mechanical properties of human bone than previously hypothesized. However, this study emphasizes the need for further research to explore the relationship between AGE accumulation and bone quality. Understanding this relationship is crucial for developing strategies to reduce fracture risk in populations with high AGE levels, such as diabetic and elderly individuals.

1. Introduction

The National Diabetes Statistics Report from 2021 states that 38.4 million Americans, 11.6 % of the U.S. population, are living with diabetes (CDC, 2024). Along with an increased risk of cardiovascular disease, chronic kidney disease, neuropathy, and lower-extremity amputations, diabetes has been shown to increase fracture risk. Individuals with type II diabetes (T2D) have up to a 69 % increased risk of bone fracture, despite having normal or even elevated BMD (Oei et al., 2013). This observation highlights that factors other than BMD are contributing to the increased fracture risk reported in T2D patients.

The accumulation of advanced glycation end products (AGEs) in diabetic bone has been theorized to compromise bone quality and contribute to the elevated fracture susceptibility in T2D patients (Saito and Marumo, 2015; Neumann et al., 2014). AGEs are the products of nonenzymatic reactions between reducing sugars, reducing proteins, lipids, or nucleic acids (Prasad et al., 2017; Asadipooya and Uy, 2019).

AGEs are produced in vivo as a result of normal metabolic processes, and gradually accumulate in tissues, including bone, with aging. However, in conditions like T2D, elevated sugar levels in blood and other body fluids lead to significantly higher AGE levels (Prasad et al., 2017). Since AGEs form through glycation events, diabetes is often diagnosed and monitored by measuring the average concentration of glycated hemoglobin (HbA1c) in the blood (The A1C Test and Diabetes - NIDDK, 2024). Studies suggest that AGEs interact with receptors on bone cells, such as osteoblasts and osteoclasts, to alter intracellular signaling and gene expression, which could disrupt the bone remodeling process (Neumann et al., 2014; Asadipooya and Uy, 2019). It has been proposed that nonenzymatic crosslinks within bone's collagen, due to AGE accumulation, stiffen bone's collagen network, leading to tissue embrittlement, and increasing the likelihood of a fracture (Murray and Coleman, 2019). If a decline in bone quality and increase in fracture risk can definitively be connected to AGE accumulation in diabetic patients, researchers could begin to develop methods to prevent AGE accumulation in bone or break

^{*} Corresponding author at: Weldon School of Biomedical Engineering, Purdue University, Indianapolis, IN, USA. *E-mail address*: jwalla78@purdue.edu (J.M. Wallace).

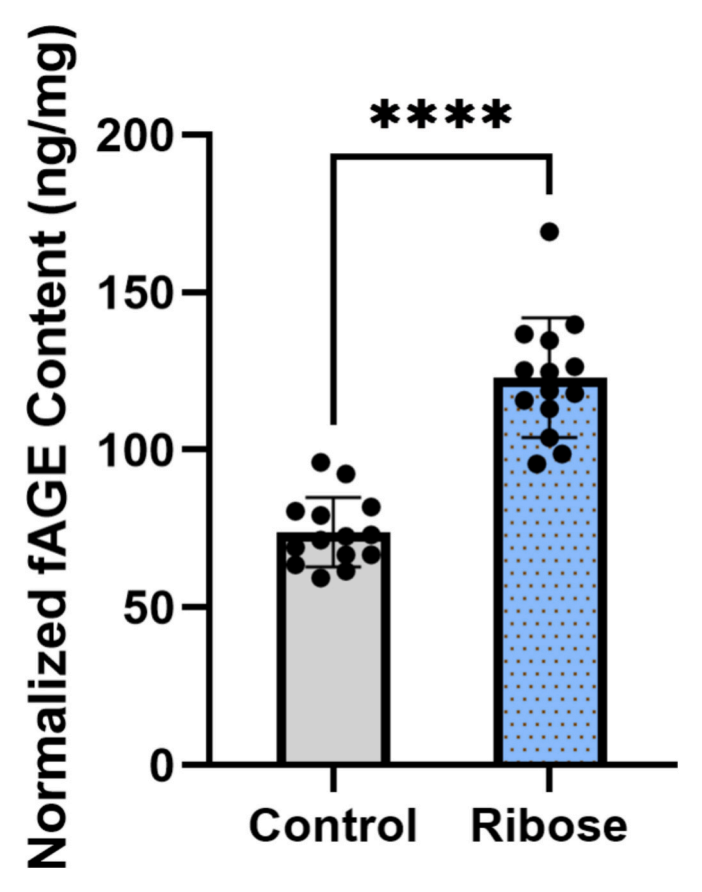


Fig. 1. Normalized fAGE Content measurements between groups. Data are presented as mean \pm standard deviation. The control group is presented in grey, and the ribose group is shown in blue speckles. Statistically significant differences (P < 0.0001) from the unpaired t-tests between groups are shown as * .

AGEs that have formed. Consequently, fracture risk could be reduced in an already vulnerable patient population. However, whether AGEs are truly driving increased fracture susceptibility in T2D patients remains contested and must be explored further. To address this, a study exploring the mechanical impacts of AGE accumulation in human cortical bone beams was executed. Beams of equal dimensions were created from the femoral shaft of a human donor. Half of these beams were incubated for 2 weeks in a ribose solution to induce AGE accumulation while the other half were placed in a control solution. It was hypothesized that with an increase in AGEs, there would be an analogous increase in bone brittleness (reflected by reduced post-yield deformation and altered viscoelasticity).

2. Material and methods

2.1. Bone samples and beam development

Bone beams were cut from a human femur (65-year-old, male) obtained from the Indiana University School of Medicine (IUSM) Anatomical Donation Program. Using an IsoMet low speed sectioning saw (Buehler, Lake Bluff, Illinois) with a diamond wafering blade, two cylindrical sections approximately 35 mm in length were cut from the femur shaft, starting from the distal end of the shaft and moving in the proximal direction. The two sections were wrapped in phosphate buffered saline (PBS)-soaked gauze and stored at $-20\,^{\circ}\mathrm{C}$ following sectioning. To cut beams from these sections, they were first thawed for approximately 1 h in a 37 $^{\circ}\mathrm{C}$ water bath. Once thawed, the bone marrow was removed using a small stainless-steel spatula. The spatula was used to gently push the tissue out of the marrow cavity. The tissue was

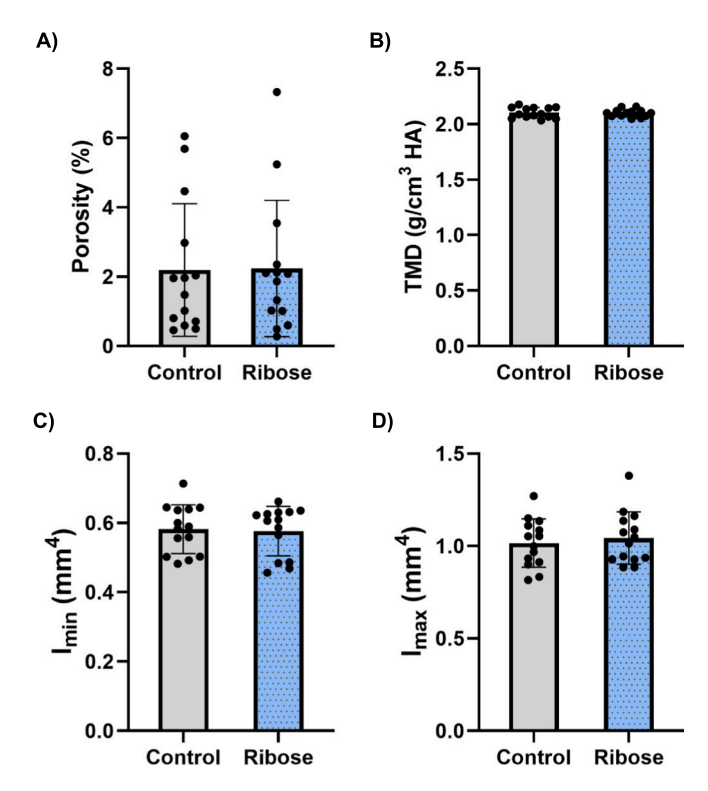


Fig. 2. (A) Porosity, (B) TMD, (C) I_{min} , and (D) I_{max} , measurements obtained from μ CT analysis. Data are presented as mean \pm standard deviation. The control group is presented in grey, and the ribose group is shown in blue speckles. Statistically significant differences (P < 0.05) from the unpaired t-tests between groups are shown as *.

Table 1 Structural-Level Mechanical Properties.

	Control	Ribose	P Value
Yield Force (N)	21.5 ± 2.7	22.01 ± 2.94	0.64
Ultimate Force (N)	25.7 ± 3.2	26.96 ± 3.63	0.34
Displacement to Yield (µm)	433.4 ± 18.5	426.29 ± 31.83	0.47
Total Displacement (μm)	828.5 ± 153.4	838.5 ± 100.4	0.84
Work to Yield (mJ)	5.11 ± 0.8	5.1 ± 0.98	0.98
Post-yield Work (mJ)	9.69 ± 4.03	10.66 ± 3.49	0.50
Total Work (mJ)	14.8 ± 3.98	15.75 ± 3.73	0.52

Data are shown as mean \pm standard deviation.

discarded after removal. An IsoMet low speed saw was used to partition the femur section into initial beams of 2.5 \times 3 \times 35 mm, then 400 grit silicon carbide sandpaper (QATM, Mammelzen, Germany) was used to uniformly shape the bone beams to nominal dimensions of $1.5 \times 2 \times 35$ mm. To ensure each beam was uniform, several thickness measurements were taken along the length of the beam in each dimension using digital calipers (VWR avantar, Radnor, Pennsylvania), discarding any beams with any dimension 10 % or more away from nominal. Each bone beam was then notched on one of the 2 mm ends by sanding the chosen end at an angle to ensure each bone was placed in a consistent orientation for mechanical testing and to provide a consistent side for measuring break length following 3-point bending tests to failure. The finished bone beams were individually wrapped in PBS-soaked gauze and stored at −20 °C. This process was repeated for all femur sections to yield a total of 28 bone beams for analysis. All samples were obtained from the same femur to prevent inter-specimen variation.

2.2. Micro computed tomography (µCT) scanning and analysis

Each bone beam was scanned using a high-resolution scanner

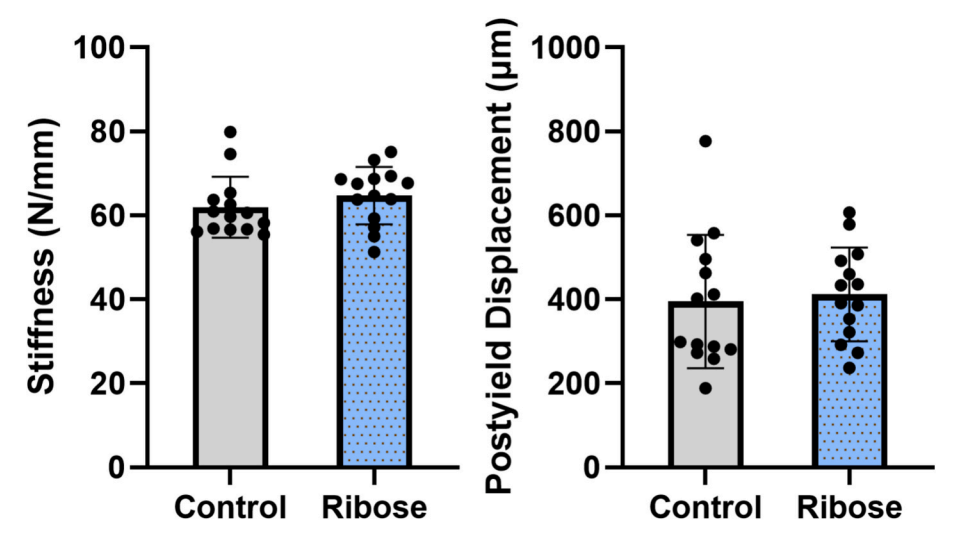


Fig. 3. Stiffness and post-yield displacement measurements obtained from three-point bending. Data are presented as mean \pm standard deviation. The control group is presented in grey, and the ribose group is shown in blue speckles. Statistically significant differences (P < 0.05) from the unpaired t-tests between groups are shown as \star .

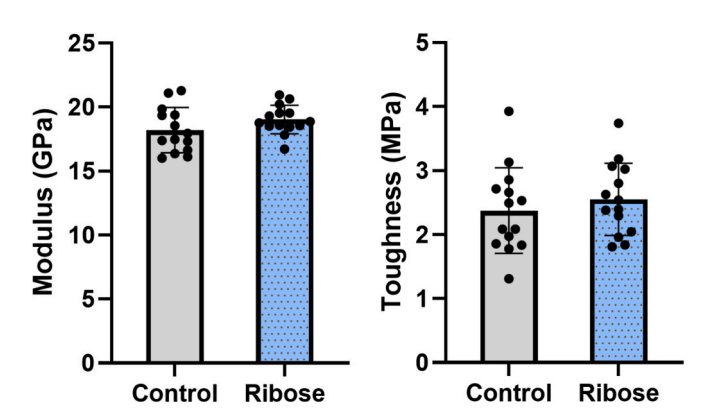


Fig. 4. Modulus and toughness measurements obtained from three-point bending and standard engineering equations. Data are presented as mean \pm standard deviation. The control group is presented in grey, and the ribose group is shown in blue speckles. Statistically significant differences (P < 0.05) from the unpaired t-tests between groups are shown as *.

Table 2 Tissue-Level Mechanical Properties.

	Control	Ribose	P Value
Yield Stress (MPa)	146.92 ± 11.04	151.9 ± 13.38	0.21
Ultimate Stress (MPa)	175.71 ± 15.49	185.8 ± 13.99	0.45
Strain to Yield (με)	$10{,}114\pm550$	$10,\!008\pm747$	0.94
Total Strain (με)	$19,\!364 \pm 3784$	$19{,}755 \pm 2907$	0.76
Resilience (MPa)	0.81 ± 0.08	0.83 ± 0.13	0.76

Data are shown as mean \pm standard deviation.

(Bruker-MicroCT 1272, Kontich, Belgium). These scans were performed at a 10 μ m voxel size, 1 mm Al filter (V = 80 kV, I = 125 μ A), 0.7-degree step angle, and a frame averaging of 2 (Kohler et al., 2021; Hatch et al., 2022). Cylindrical hydroxyapatite phantoms (0.3 and 1.25 g/cm³ Ca-HA) were scanned once for the study to evaluate tissue mineral

density (TMD) of the scanned bone beams. Once scanned, the samples were stored in PBS-soaked gauze at $-20\,^{\circ}$ C.

SkyScan softwares (NRecon and DataViewer) (Bruker, Billerica, MA) were used to reconstruct and rotate the bone beam scans to obtain a consistent orientation of all beams prior to analysis. Using CTAn (Bruker, Billerica, MA), eleven slices were selected, centered at the 50 % region of the beam and saved for analysis. These regions of interest (ROIs) were analyzed using a custom MATLAB (MathWorks, Natick, MA) script to obtain cortical TMD, then analyzed in CTAn to quantify porosity. The area of the ROIs for each of the bone beams was calculated using a custom MATLAB script to ensure the dimensions of the beam were within a 10 % error range. μ CT analysis was completed before separating the samples into experimental groups to ensure samples had uniform cross sections and those with significant porosities were distributed equally throughout groups.

2.3. In-vitro solution incubation

Following uCT analysis, bone beams were randomly sorted into one control group and one ribose group (n = 14 per group). The base soaking solution was comprised of 5 mM Benzamidine (Sigma-Aldrich, St. Louis, MO), 10 mM N-ethylmaleimide (NEM) (Sigma-Aldrich), 30 mM HEPES (Sigma-Aldrich), 0.5 M CaCl2 (Sigma-Aldrich), 1 x Pen-Strep (Sigma-Aldrich), and Hanks Balanced Salt Solution (HBSS) (Fisher Scientific, Waltham, Massachusetts) as the solvent (Vesper et al., 2017). Pen-strep was added to each solution to prevent any bacterial growth that could harm the quality of the samples. Protease inhibitors and calcium chloride were added to prevent collagen degradation and mineral loss, respectively. The control group was soaked in the base solution, while the experimental group was soaked in the base solution supplemented with ribose at a concentration 0.6 M. Each bone beam was placed individually in a labeled 5 mL tube and the respective solutions were divided among the 5 mL tubes. The individual tubes were taped onto a nutator and soaked for a total of 15 days in a warm room at 37 °C. The solution was changed every 2-3 days.

2.4. Mechanical analysis

2.4.1. Dynamic mechanical analysis (DMA)

Following soaking, an ElectroForce 3200 High Force DMA (TA Instruments, New Castle, DE, USA) tester equipped with a 225 N load cell was used to cyclically load the bone beams and analyze loss modulus and storage modulus. A three-point bending setup was used with a

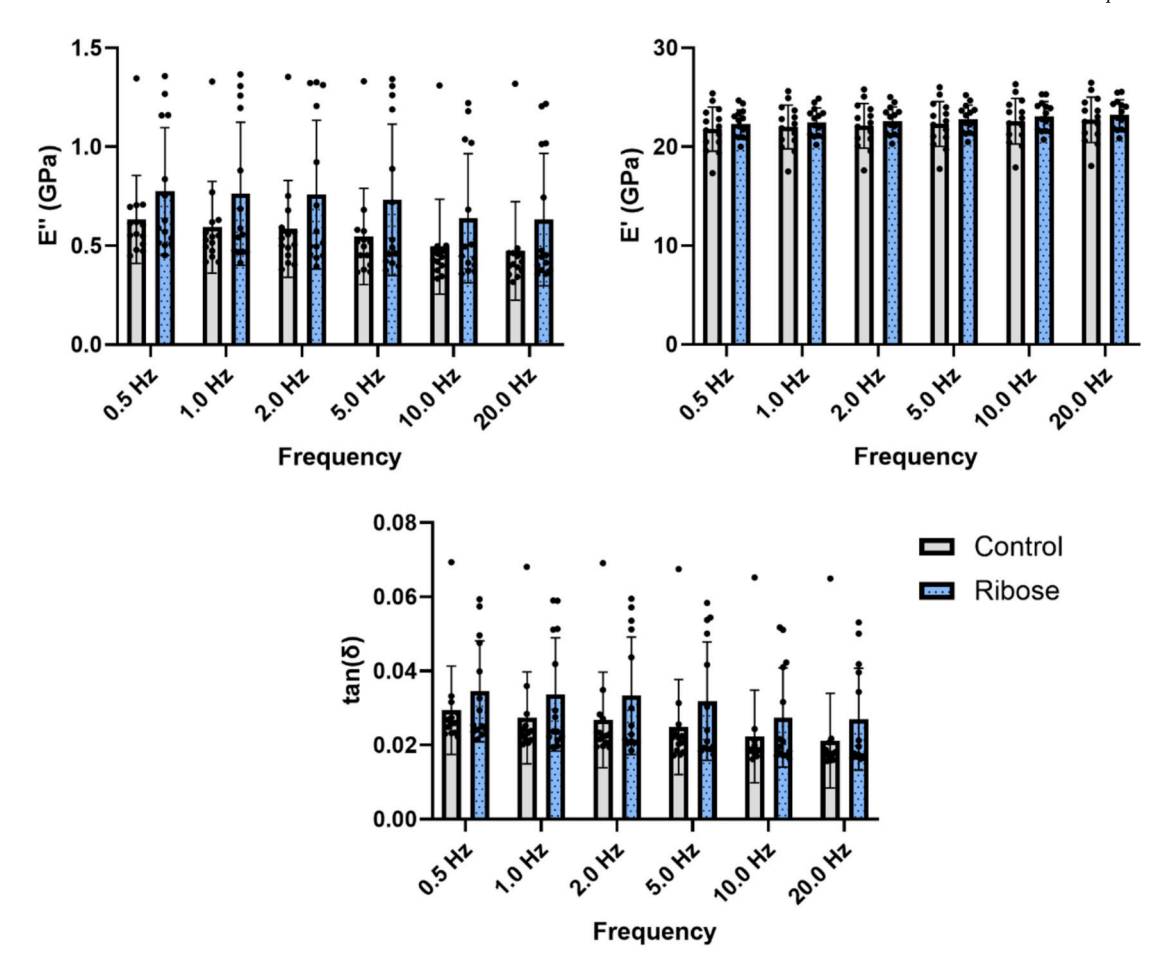


Fig. 5. Loss modulus (E"), storage modulus (E'), and tan(δ) measurements at various frequencies obtained from DMA. Data are presented as mean \pm standard deviation. The control group is presented in grey, and the ribose group is shown in blue speckles. Statistically significant differences (P < 0.05) from the unpaired t-tests between groups are shown as *.

support span of 19.5 mm, a 5 N static load, and a 2 N dynamic load. To account for the dynamic response of the machine, a calibration procedure was performed using a tungsten bar to measure the compliance of the machine and fixture setup prior to testing. This machine compliance was then automatically accounted for during measurement and collection of data. The loads on the bone beams were minimal and remained in the lower portion of the linear elastic region to prevent plastic deformation during testing. DMA testing began at the lowest testing frequency, then gradually increased to the maximum testing frequency using the following frequencies: 0.5 Hz, 1 Hz, 2 Hz, 5 Hz, 10 Hz, then 20 Hz. After ramping up in frequency, the test protocol ramped down through the same frequency values in reverse order. This frequency range was selected based on published load rise times during walking. The rise time from heel strike to peak load in the hip joint has been shown to be in the range of 100-150 ms during walking, corresponding to a frequency of 3.3-5 Hz (Bergmann et al., 1993). This range does not cover the entirety of physiologically relevant loading times (particularly the fast loading rates associated with impact events), but it does cover a range associated with everyday activity, making it appropriate for this application. Samples were tested in open air at the same temperature as the laboratory environment (\sim 21 $^{\circ}$ C) and hydrated throughout testing using a vaporizer filled with purified Milli-Q water. The resulting data were analyzed to quantify the viscoelastic properties of the bone.

2.4.2. Three-point bending tests to failure

Following DMA, three-point bending tests to failure were conducted using an ElectroForce 5500 Mechanical Tester (TA Instruments, New Castle, DE, USA) to evaluate the structural and estimated tissue level

mechanical properties of the bone beams. These tests were performed using a 225 N load cell at a displacement rate of 0.025 mm/s in displacement control. The support span of the test was set to 20 mm and beams were oriented such that the loading point contacted the midpoint of the beam. A preload of 0.25 N was placed on each bone beam to ensure it did not move throughout the mechanical test. Following failure, the length from the notched end of the beam to the break point was measured. This length measure was used to produce μCT ROIs centered about the break point for each beam (20 slices total). These ROIs were then analyzed using a custom MATLAB script to obtain geometric properties of the beams at the break point, needed to convert the recorded force and displacement data to stress and strain, respectively, using standard engineering Eqs. (Wallace et al., 2009). Another custom MATLAB script was used to obtain structural level and material level mechanical properties.

To identify the yield point, the 0.2 % offset method was used. A line parallel to the elastic region of the stress-strain curve was generated and offset by 0.2 % strain then plotted alongside the stress-strain curve (Reul et al., 2023). The x and y coordinate of the intersection of this line with the stress-strain curve is considered the yield point, strain to yield (x) and yield stress (y). Displacement to yield (x) and yield force (y) values could then be found using the coordinates of the yield point.

2.5. Fluorescent advanced glycation end product (fAGE) analysis

Following bending tests, broken bone beams were prepared for fAGE analysis. Beams were first demineralized using ethylenediaminetetra-acetic acid (EDTA) over nine days with the solution being changed every

other day. Demineralization was verified from a dual x-ray absorptiometry (DEXA) scan. Once demineralized, the samples were dried for 24 h at 37 °C before measuring and recording each sample's dry weight. The samples were then hydrolyzed in hydrochloric acid (HCl) at 110 $^{\circ}$ C for 20 h. The HCl was removed using a SpeedVac (Thermo Fisher Scientific, SPD140DDA, Waltham, MA, USA). Following HCl removal, samples were resuspended in High Performance Liquid Chromatography (HPLC)-grade water to yield a concentration of 50 $\frac{\mu g}{mL}$ (based on dry weight), then filtered using a Nylon syringe filter with 0.2 um pore size (Fisher Scientific, Waltham, Massachusetts) into a new sample tube. A volume of 100 µL was removed from these samples for the hydroxyproline assay before the remaining volume, designated for fAGE analysis, was placed in the SpeedVac to remove the water. The samples designated for fAGE analysis were resuspended in sulfuric acid to obtain a concentration of 10.9 $\frac{mg}{mL}$. A volume of 65 μ L of the resuspended samples were plated in duplicate in a 96-well plate, along with quinine sulfate standards (10, 8, 6, 5, 4, 3, 2, 1, $0 \frac{\mu g}{ml}$). The fluorescence of these samples and standards were measured using a Spark Multimode Microplate Reader (Tecan, Männedorf, Switzerland) with an excitation wavelength of 370 nm and emission wavelength of 440 nm. A standard curve was generated from the quinine sulfate standards and used to calculate the AGE concentration of each sample given the measured fluorescence.

A hydroxyproline assay was then performed using the aliquoted 100 μ L to determine the collagen content in each sample for normalization of AGE content to collagen content. The hydroxyproline assay was carried out using the quantichrome hydroxyproline assay kit (DHYP-100) (BioAssay Systems, Hayward, California). The standards and samples were plated in duplicate in a 96-well plate and read at a wavelength of 560 nm. The calculated hydroxyproline concentrations were then converted to collagen concentration, assuming 13 % of collagen was hydroxyproline (Dull and Henneman, 1963).

2.6. Statistical analysis

To evaluate whether statistically significant differences between the control and ribose groups existed, unpaired t-tests were performed for all measured parameters. PRISM 10.2.3 (GraphPad Software, La Jolla California, USA) was used to perform all statistical analysis with a significance level set at 0.05. If statistically significant differences are detected, these will be denoted in figures using *. All data in figure and tables are represented as mean \pm standard deviation (SD).

3. Results

3.1. fAGE Analysis

The findings from the fAGE analysis show that soaking in ribose led to a statistically significant elevation in normalized fAGE mass between groups (Fig. 1).

3.2. µCT analysis

 μCT measurements for both the control and ribose-treated groups are displayed in Fig. 2. There were no significant differences observed between the groups for any of the μCT parameters. As noted in the methods, the porosity and TMD values were kept consistent between the groups, while I_{max} and I_{min} confirm that there are no significant differences in the size and shape of the bone beams.

3.3. Mechanical analysis

3.3.1. Three-point bending analysis

Structural-level mechanical properties measured by three-point bending tests are presented in Table 1 and Fig. 3. Despite trends

toward greater stiffness and post-yield displacement in the ribose-treated group (Fig. 3), none of the structural-level mechanical properties were significantly different between groups (Table 1). Estimated tissue-level mechanical properties were calculated using standard engineering equations. Similar to the structural-level results, the ribose group demonstrated trends toward higher modulus and toughness (Fig. 4), but none of the tissue-level mechanical properties were significantly different between groups (Table 2).

3.3.2. Dynamic mechanical analysis

The DMA data reveal no significant differences between groups in loss modulus (E"), storage modulus (E'), or $tan(\delta)$ at any tested frequency (Fig. 5).

4. Discussion

There is a limited literature base on the mechanical impacts of AGE accumulation, particularly in human cortical bone. While studies in rodent bone have found differences in mechanical properties with AGE accumulation, the results of the current study suggest those findings may not extend to human cortical bone.

4.1. AGE accumulation does not correlate with significant mechanical differences

This study found no significant differences in any of the mechanical properties analyzed in ribose-soaked samples, despite elevated AGE levels. It is important to acknowledge that the ribose soaking method used in this study does not directly replicate in-vivo AGE accumulation. The effects of AGE accumulation may differ between living bone, which undergoes constant turnover, and in-vitro soaking of bone samples. This distinction could potentially explain the lack of significant differences in mechanical properties. Additionally, while in-vivo AGE accumulation can be induced by elevated glucose in the bloodstream, this study used ribose to induce AGE formation more rapidly (Ban et al., 2022; Sroga et al., 2015). A key mechanism involved in in-vivo AGE accumulation is the cross-linking of collagen through the glycation of its free amino acids (Luevano-Contreras and Chapman-Novakofski, 2010). This AGEinduced cross-linking of collagen has been proposed to lead to increased rigidity and altered mechanical properties over time (Luevano-Contreras and Chapman-Novakofski, 2010). Given this mechanism, the rapid formation of AGEs using ribose in this study may not fully replicate the in-vivo effects of glucose-induced AGE accumulation because it may not allow enough time for the collagen crosslinking process. The slower, more gradual accumulation of AGEs invivo may allow for more significant structural and functional changes in collagen, which could be necessary for observing changes in cortical bone mechanical properties. Another explanation for the lack of significant differences between groups could be the presence of an AGE threshold. Since AGEs accumulate naturally in bone over time, and the human bone sample used was from a 65-year-old individual, it is possible that the existing level of AGEs had already compromised the material properties of the bone to a degree where additional AGE accumulation did not produce further degradation.

4.2. Role of DMA in mechanical analysis

DMA was implemented to characterize the viscoelastic properties of the bone samples because it can describe the relaxation of the polymer chains of a material (Menard and Menard, 2020). This description of the material is key because AGEs are known to impact the collagen network in bone, meaning this method may be more sensitive than other techniques used to detect mechanical changes induced by AGEs. During DMA testing, a sinusoidal oscillatory stress is applied to samples that causes sinusoidal deformation, measured as strain (2.10: Dynamic Mechanical Analysis, 2024). The phase difference between the applied

stress and measured strain is what characterizes the viscoelastic properties of the material (2.10: Dynamic Mechanical Analysis, 2024). For ideal elastics, the phase angle between stress and strain is 0°, whereas for a viscous material, the applied stress leads the strain by 90°. Viscoelastic materials have a phase lag between 0° and 90°. Important parameters in DMA data analysis include loss modulus, storage modulus, and $tan(\delta)$, which represent the viscous component, elastic component, and viscoelastic damping of the material, respectively (2.10: Dynamic Mechanical Analysis, 2024). DMA tests often adjust the temperature of the sample or oscillation frequency to analyze how these variables affect the DMA parameters. In this study, DMA testing was used to analyze the effect of oscillation frequency on viscoelastic properties in the control and ribose groups. It was hypothesized that increased levels of AGEs in the ribose group would lead to a stiffer, more brittle bone, resulting in a decrease in $tan(\delta)$ due to an increase in storage modulus. As expected, the storage modulus (E') was elevated at all frequencies in the ribose group compared to the control group but failed to reach significance. The loss modulus (E") and $tan(\delta)$ also trended higher in the ribose group, which was not expected. These findings suggest that the mechanical impacts of AGE accumulation in bone may be more complex than expected.

4.3. Limitations

Using fAGEs to measure total AGE content may not capture the presence of all AGEs since not all AGEs are fluorescent. Measuring total AGE content and assessing specific AGEs (pentosidine, carboxymethyl lysine, etc.) could provide an understanding of the accumulation of a variety of AGEs, yielding a more comprehensive understanding of the differences between groups. However, fAGEs were measured in this study because the assay kit used is a reliable and accessible method, while other methods for quantifying total AGEs or specific AGEs are less readily available, more labor intensive, and still may not comprehensively capture all AGEs present in bone. Nonetheless, the significant elevation of fAGEs in the ribose group compared to the control group suggests that glycation events did occur in the ribose-soaked samples.

4.4. Conclusion and future directions

Although this study did not find significant mechanical differences due to AGE accumulation in human cortical bone, it highlights the need for further research. Understanding the role of AGEs on bone quality is critical for developing strategies to mitigate fracture risk in populations with high AGE levels, such as diabetic and elderly individuals. Future research should continue to explore the relationship between AGE accumulation and bone mechanical properties in human samples, potentially using bone from younger individuals, different bone locations, or measuring other AGEs along with fluorescent AGEs.

CRediT authorship contribution statement

Katelynn R. Gallagher: Conceptualization, Formal analysis, Writing – original draft, Writing – review & editing. Olivia N. White: Conceptualization, Formal analysis, Investigation, Methodology, Writing – review & editing. Andrew A. Tomaschke: Methodology, Writing – review & editing. Dyann M. Segvich: Conceptualization, Supervision, Writing – review & editing. Joseph M. Wallace: Conceptualization, Formal analysis, Funding acquisition, Methodology, Project administration, Supervision, Writing – review & editing.

Declaration of competing interest

The authors declare no conflict of interest.

Acknowledgements

This work was supported by the National Institutes of Health (JMW grant no. RO1 AR072609; AAT grant no. T32 AR065971) and the National Science Foundation (JMW; grant no. 1952993).

Data availability

Data will be made available on request.

References

- "2.10: Dynamic Mechanical Analysis," Chemistry LibreTexts. Accessed: Sep. 25, 2024. [Online]. Available: https://chem.libretexts.org/Bookshelves/Analytical_Chemistry/Physical_Methods_in_Chemistry_and_Nano_Science (Barron)/02%3A_Physical_and_Thermal_Analysis/2.10%3A_Dynamic_Mechanical_Analysis.
- Asadipooya, K., Uy, E.M., 2019. Advanced glycation end products (AGEs), receptor for AGEs, diabetes, and bone: review of the literature. J. Endocr. Soc. 3 (10), 1799–1818. https://doi.org/10.1210/js.2019-00160.
- Ban, I., Sugawa, H., Nagai, R., 2022. Protein modification with ribose generates Nδ-(5-hydro-5-methyl-4-imidazolone-2-yl)-ornithine. Int. J. Mol. Sci. 23 (3), 1224. https://doi.org/10.3390/ijms23031224.
- Bergmann, G., Graichen, F., Rohlmann, A., 1993. Hip joint loading during walking and running, measured in two patients. J. Biomech. 26 (8), 969–990. https://doi.org/ 10.1016/0021-9290(93)90058-m.
- CDC, 2024. National Diabetes Statistics Report. Diabetes. Accessed: Jun. 25 [Online]. Available: https://www.cdc.gov/diabetes/php/data-research/index.html.
- Dull, T.A., Henneman, P.H., 1963. Urinary Hydroxyproline as an index of collagen turnover in bone. N. Engl. J. Med. 268 (3), 132–134. https://doi.org/10.1056/ NEJM196301172680305.
- Hatch, J.M., Segvich, D.M., Kohler, R., Wallace, J.M., 2022. Skeletal manifestations in a streptozotocin-induced C57BL/6 model of type 1 diabetes. Bone Rep. 17, 101609. https://doi.org/10.1016/j.bonr.2022.101609.
- Kohler, R., et al., 2021. The effect of single versus group μCT on the detection of trabecular and cortical disease phenotypes in mouse bones. JBMR Plus 5 (4), e10473. https://doi.org/10.1002/jbm4.10473.
- Luevano-Contreras, C., Chapman-Novakofski, K., 2010. Dietary advanced glycation end products and aging. Nutrients 2 (12), 1247–1265. https://doi.org/10.3390/ pu2121247
- Menard, K., Menard, N., 2020. Dynamic mechanical Analysis. https://doi.org/10.1201/ 9780429190308.
- Murray, C.E., Coleman, C.M., 2019. Impact of diabetes mellitus on bone health. Int. J. Mol. Sci. 20 (19), 4873. https://doi.org/10.3390/ijms20194873.
- Neumann, T., et al., 2014. High serum pentosidine but not esRAGE is associated with prevalent fractures in type 1 diabetes independent of bone mineral density and glycaemic control. Osteoporos. Int. 25 (5), 1527–1533. https://doi.org/10.1007/ s00198-014-2631-7.
- Oei, L., et al., 2013. High bone mineral density and fracture risk in type 2 diabetes as skeletal complications of inadequate glucose control: the Rotterdam study. Diabetes Care 36 (6), 1619–1628. https://doi.org/10.2337/dc12-1188.
- Prasad, C., Davis, K.E., Imrhan, V., Juma, S., Vijayagopal, P., 2017. Advanced glycation end products and risks for chronic diseases: intervening through lifestyle modification. Am. J. Lifestyle Med. 13 (4), 384–404. https://doi.org/10.1177/ 1559827617708991.
- Reul, O.N., Anneken, A.M., Kohler, R.K., Segvich, D.M., Wallace, J.M., 2023. Practical considerations for the design, execution, and interpretation of studies involving whole-bone bending tests of rodent bones. J. Vis. Exp. JoVE 199. https://doi.org/ 10.3791/65616.
- Saito, M., Marumo, K., 2015. Effects of collagen crosslinking on bone material properties in health and disease. Calcif. Tissue Int. 97 (3), 242–261. https://doi.org/10.1007/ s00223-015-9985-5.
- Sroga, G.E., Siddula, A., Vashishth, D., 2015. Glycation of human cortical and cancellous bone captures differences in the formation of Maillard reaction products between glucose and ribose. PLoS One 10 (2), e0117240. https://doi.org/10.1371/journal. pone.0117240.
- "The A1C Test & Diabetes NIDDK," National Institute of Diabetes and Digestive and Kidney Diseases. Accessed: Jul. 21, 2024. [Online]. Available: https://www.niddk.nih.gov/health-information/diagnostic-tests/a1c-test.
- Vesper, E.O., Hammond, M.A., Allen, M.R., Wallace, J.M., 2017. Even with rehydration, preservation in ethanol influences the mechanical properties of bone and how bone responds to experimental manipulation. Bone 97, 49–53. https://doi.org/10.1016/j.bone.2017.01.001.
- Wallace, J.M., Golcuk, K., Morris, M.D., Kohn, D.H., 2009. Inbred strain-specific response to Biglycan deficiency in the cortical bone of C57BL6/129 and C3H/he mice. J. Bone Miner. Res. 24 (6), 1002–1012. https://doi.org/10.1359/jbmr.081259.